(^4S) limit, and their possible combinations with other terms built on the same limit lie at too long wave-lengths to be photographed. The combinations that are observed are all relatively weak, and although some of the unclassified lines are probably due to other terms of this configuration, it is not possible to identify them at present.

Two lines are observed having wave numbers agreeing with the differences of certain $4p^4$ terms; namely, ${}^1D_2-{}^1S_0$ and ${}^3P_1-{}^1S_0$. The former of these fits equally well as a $({}^4S)5p\,{}^3P_2-({}^4S)6d\,{}^5D_3$ intercombination, several other lines of which are also found, and this seems to be the more reasonable assignment. The latter, however, has no other place in the present term scheme except as this transition.

Table II contains all the known Se I terms with their numerical values referred to the ^4S state of the ion as zero. Those terms which are known to perturb each other are listed under their predominating configurations and with a common number in the parentheses to show the sharing configuration of each.

NOVEMBER 15, 1934 PHYSICAL REVIEW VOLUME 46

The Paschen-Back Effect. II. *JJ*-Coupling (approx.)

J. B. Green and R. A. Loring,* *Mendenhall Laboratory of Physics*

(Received September 24, 1934)

The Paschen-Back effect of four pairs of *mercury* lines, λλ5789–90, 3662–63, 3131–32 and 2967–68, have been measured. The results have been found to be in good agreement with Houston's theory, both as to position and intensities of components. *The red shift* of the central component of λ5790 was studied in greater detail at several field strengths and was found to be practically proportional to the square of the field strengths. *The Zeeman effect* of several other mercury lines was also measured, and the g-values calculated from them were slightly different from the normal g-values, but are in general accord with the values calculated from perturbation theory.

In a previous communication,[1] the incomplete Paschen-Back effect of the Zn and Cd ${}^3P{}^3D$ multiplet was discussed. The agreement between Darwin's[2] calculations and experiment were very satisfactory. In Darwin's work, the effect of electrostatic interaction between the two electrons was neglected, so that the results could be expected to be satisfactory only for LS-coupling. The $sd\,{}^3D$ and $sd\,{}^1D$ terms of both Zn and Cd are sufficiently separated so that this approximation was valid. But in the case of Hg, the $6s4d\,{}^3D_1$ and ${}^1D_2$ are only 3 cm^{-1} apart, and in even moderately strong magnetic fields perturbing effects become quite large. Four groups of lines involving these two levels and the $6s6p\,{}^3P$ and ${}^1P$ levels, namely λλ5789–90, 3662–3, 3131–32, and 2967–68, were studied, with a view to comparing the experimental results with the theory of singlets and triplets developed by Houston.[3]

Houston has calculated the matrix elements of the interaction of two electrons (one an s-electorn) with an external magnetic field and has completed the calculations for weak fields, i.e., to first order terms. In our work we found that this method would not be sufficiently accurate even for our weakest fields, so that it was necessary to use the complete secular determinant of Houston and not to neglect the second and third order terms.

If $\psi=a_1\varphi_1+a_2\varphi_2+a_3\varphi_3+a_4\varphi_4$ be the zero-order approximation of the wave function where

* Assistant Professor of Physics, University of Louisville, Louisville, Ky.

[1] Green and Gray, Phys. Rev. **45**, 273 (1934).

[2] Darwin, Proc. Roy. Soc. **A115**, 1 (1927).

[3] Houston, Phys. Rev. **33**, 297 (1929).

$$\varphi_1=A/\{2[(l-m)!]^{\frac{1}{2}}[(l+m)!]^{\frac{1}{2}}\}\{P_l^m(2)+P_l^m(1)\}\{S_\alpha(1)S_\beta(2)-S_\beta(1)S_\alpha(2)\},$$
$$\varphi_2=A/\{2^{\frac{1}{2}}[(l-m+1)!]^{\frac{1}{2}}[(l+m-1)!]^{\frac{1}{2}}\}\{P_l^{m-1}(2)-P_l^{m-1}(1)\}S_\alpha(1)S_\alpha(2),$$
$$\varphi_3=A/\{2[(l-m)!]^{\frac{1}{2}}[(l+m)!]^{\frac{1}{2}}\}\{P_l^m(2)-P_l^m(1)\}\{S_\alpha(1)S_\beta(2)+S_\beta(1)S_\alpha(2)\},$$
$$\varphi_4=A/\{2^{\frac{1}{2}}[(l-m-1)!]^{\frac{1}{2}}[(l+m)!]^{\frac{1}{2}}\}\{P_l^{m+1}(2)-P_l^{m+1}(1)\}S_\beta(1)S_\beta(2),$$

the first part of the product being a function of the coordinates of the two electrons, and the second part a function of the spin. A is a function of l alone.

The secular equation then takes the form

$$\begin{vmatrix} X+\omega m-E & -2^{-\frac{1}{2}}[(l+m)(l-m+1)]^{\frac{1}{2}} & -m & 2^{-\frac{1}{2}}[(l-m)(l+m+1)]^{\frac{1}{2}} \\ -2^{-\frac{1}{2}}[(l+m)(l-m+1)]^{\frac{1}{2}} & \{\omega(m+1)+m-1-E\} & -2^{-\frac{1}{2}}[(l+m)(l-m+1)]^{\frac{1}{2}} & 0 \\ -m & -2^{-\frac{1}{2}}[(l+m)(l-m+1)]^{\frac{1}{2}} & \omega m-E & -2^{-\frac{1}{2}}[(l-m)(l+m+1)]^{\frac{1}{2}} \\ 2^{-\frac{1}{2}}[(l-m)(l+m+1)]^{\frac{1}{2}} & 0 & -2^{-\frac{1}{2}}[(l-m)(l+m+1)]^{\frac{1}{2}} & \{\omega(m-1)-m-1-E\} \end{vmatrix}=0,$$

the four solutions (in general) of E giving the positions of the energy levels in the magnetic field. When $|m|=l+1$ the determinant reduces to a single diagonal element, for then only φ_2 has a meaning, and when $|m|=l$ to a third-order determinant, for then φ_4 has no meaning. The values of E put into the original equations then serve to determine the relations between the a's, from which the intensities of the transitions may be calculated.

If these computations are carried out, the intensities of the different transitions are

$l\rightarrow l-1,\quad m\rightarrow m-1\quad$ (perpendicular polarization)

$$I\sim B\{a_{1,\,l,\,m}a_{1,\,l-1,\,m-1}[(l+m)!]^{\frac{1}{2}}/[(l+m-2)!]^{\frac{1}{2}}+a_{2,\,l,\,m}a_{2,\,l-1,\,m-1}[(l+m-1)!]^{\frac{1}{2}}/[(l+m-3)!]^{\frac{1}{2}}$$
$$+a_{3,\,l,\,m}a_{3,\,l-1,\,m-1}[(l+m)!]^{\frac{1}{2}}/[(l+m-2)!]^{\frac{1}{2}}+a_{4,\,l,\,m}a_{4,\,l-1,\,m-1}[(l+m+1)!]^{\frac{1}{2}}/[(l+m-1)!]^{\frac{1}{2}}\}^2,$$

$l\rightarrow l-1,\quad m\rightarrow m+1\quad$ (perpendicular polarization)

$$I\sim B\{a_{1,\,l,\,m}a_{1,\,l-1,\,m+1}[(l-m)!]^{\frac{1}{2}}/[(l-m-2)!]^{\frac{1}{2}}+a_{2,\,l,\,m}a_{2,\,l-1,\,m+1}[(l-m+1)!]^{\frac{1}{2}}/[(l-m-1)!]^{\frac{1}{2}}$$
$$+a_{3,\,l,\,m}a_{3,\,l-1,\,m+1}[(l-m)!]^{\frac{1}{2}}/[(l-m-2)!]^{\frac{1}{2}}+a_{4,\,l,\,m}a_{4,\,l-1,\,m+1}[(l-m-1)!]^{\frac{1}{2}}/[(l-m-3)!]^{\frac{1}{2}}\}^2,$$

$l\rightarrow l-1,\quad m\rightarrow m\quad$ (parallel polarization)

$$I\sim 4B\{a_{1,\,l,\,m}a_{1,\,l-1,\,m}[(l+m)!]^{\frac{1}{2}}[(l-m)!]^{\frac{1}{2}}/[(l+m-1)!]^{\frac{1}{2}}[(l-m-1)!]^{\frac{1}{2}}$$
$$+a_{2,\,l,\,m}a_{2,\,l-1,\,m}[(l+m-1)!]^{\frac{1}{2}}[(l-m+1)!]^{\frac{1}{2}}/[(l+m-2)!]^{\frac{1}{2}}[(l-m)!]^{\frac{1}{2}}$$
$$+a_{3,\,l,\,m}a_{3,\,l-1,\,m}[(l+m)!]^{\frac{1}{2}}[(l-m)!]^{\frac{1}{2}}/[(l+m-1)!]^{\frac{1}{2}}[(l-m-1)!]^{\frac{1}{2}}$$
$$+a_{4,\,l,\,m}a_{4,\,l-1,\,m}[(l+m+1)!]^{\frac{1}{2}}[(l-m-1)!]^{\frac{1}{2}}/[(l+m)!]^{\frac{1}{2}}[(l-m-2)!]^{\frac{1}{2}}\}^2,$$

B is a function of l alone and need not be used when considering relative intensities.

$\lambda\lambda$5789–90. This investigation was begun as a result of some correspondence with Professor Condon regarding the red shift of the central component of the 5790 line ($^1P_1-{}^1D_2$). Previous workers[4, 5, 6] had found that this shift was proportional to the square of the magnetic field, and Gmelin[4] in an exhaustive investigation studied the behavior of the 5789 line ($^1P_1-{}^3D_1$) also. Our measurements on these two lines soon showed that a second-order perturbation calculation was not sufficient to explain the anomalies observed in their behavior. Such a calculation leads one to expect a smaller effect for the perpendicular than for the parallel components of 5790, while actu-

[4] Gmelin, Phys. Zeits. **9**, 212 (1908); **11**, 1193 (1910).
[5] Zeeman, Proc. Amst. Acad. Sci. **10**, 351 (1907).
[6] Risco, Phys. Zeits. **13**, 137 (1912).

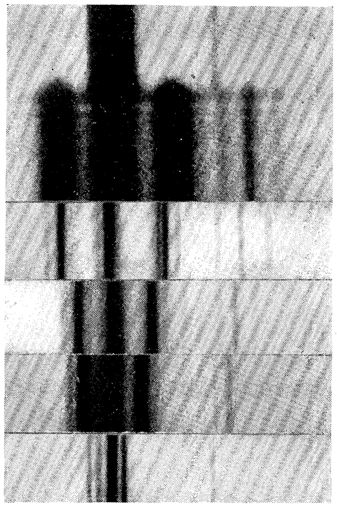

FIG. 1. $\lambda\lambda$5789–90 at different field strengths. Hg 5789 +5790. (a) no field; (b) 34,700 gauss; (c) 29,800 gauss; (d) 21,670 gauss; (e) 16,860 gauss; (f) no field.*

ally the short-wave perpendicular component splits at about 18,000 gauss (see Fig. 1).

The behavior of these two lines in the magnetic field is very interesting, although one must be very careful in any investigation of the lines of mercury. All of these lines are contaminated by the presence of hyperfine structure, and care must be taken to avoid confusion of these components with Zeeman components of the even isotopes, which show no hyperfine structure. This can only be done by taking a sequence of photographs at varying field strength and noting the positions of the lines. The effect is shown clearly in Fig. 1. The two faint lines, one on each side of the long wave component, are clearly lines due to hyperfine structure. We are concerned here only with the even isotopes and their behavior.

Fig. 2 is a typical photograph of $\lambda\lambda$5789–90 and shows the Zeeman effect at about 29,600 gauss. The lowest picture is a 7X enlargement of the second order (about 0.51 A/mm on the original negative), the middle picture the theoretical positions and intensities of the lines, and the top picture a microphotogram of the bottom picture, made by a Moll microphotometer.

If the classification of λ5790 were ${}^1P_1-{}^1D_2$ in strictly LS-coupling we should expect the pattern to be a normal triplet, but both the ${}^1P$ and ${}^1D$ levels are perturbed and the g-values are

* In all figures, the wave-length increases from right to left.

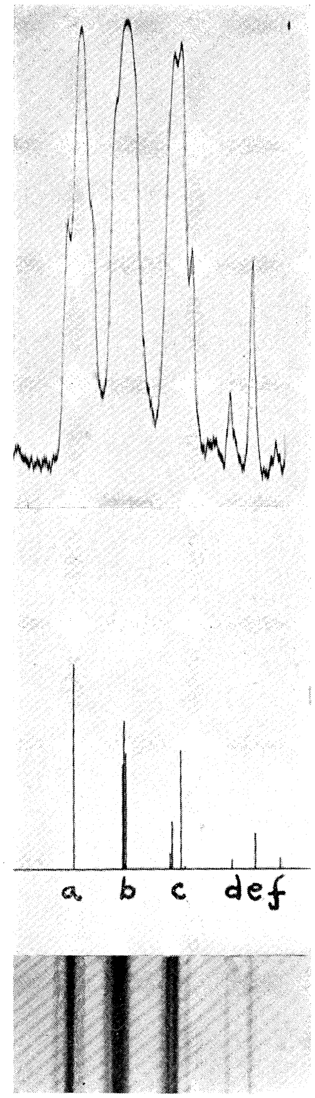

FIG. 2. $\lambda\lambda$5789–90, Field strength about 30,000 gauss.

different from unity, resulting in a splitting of each of the components into three, which is first manifested in the doubling of the component marked "c" in Fig. 2, beginning to be visible at about 20,000 gauss. This has not been noticed by other observers. Another evidence that ${}^1D$ has acquired some "triplet" character is shown by the fact that it exhibits a Paschen-Back effect. The central component "b" shifts toward the red with increasing field, while the parallel (usually forbidden component, for $\Delta J=0$, $m=0\rightarrow m=0$) component "d" of λ5789 shifts to the violet. The amount of this red shift of 5790 is shown graphi-

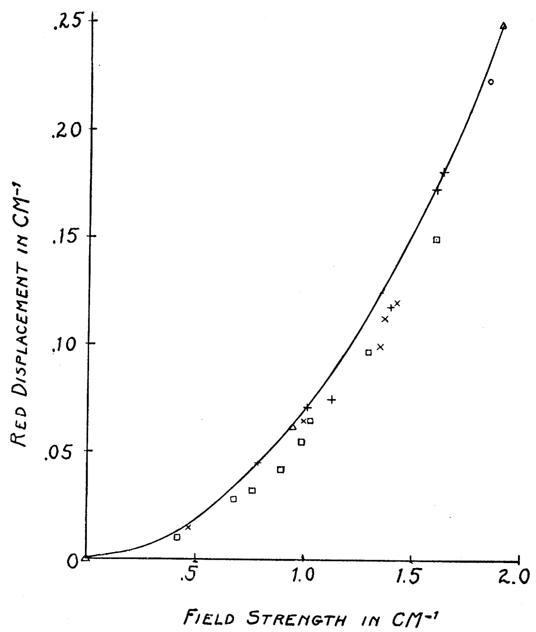

FIG. 3. Curve showing relation between red shift of central component of λ5790 and field strength. Triangle, theoretical points. The solid line is a theoretical curve. Plus, present experiment. Measured as displacement with respect to 5770. Circle, direct displacement measurement. Square, Gmelin's measurements. Cross, Risco's measurements. 1 $\mathrm{cm}^{-1}=21{,}200$ gauss.

cally in Fig. 3, together with the results of other observers. It was not possible to measure this shift directly by displacement from known iron lines, for the plate always seemed to be jarred when introducing comparison spectra. The shifts are therefore measured with reference to the central component of 5770, which did not seem to be disturbed. Gmelin and Rosco measured this displacement as half the dissymmetry of the pattern. Their results should therefore be lower than ours, because they were unable to resolve the short wave component, the outside edge of which behaves practically normally. The full curve is calculated theoretically from Eqs. (1) and (2) using the value $X=-\frac{1}{2}$ for the $^1D\,^3D$ electrostatic parameter. The results of all the observers are seen to be within experimental error, the largest observable shift being only 0.074A. The curve is practically parabolic, indicating a variation with H^2, although it eases off at the strongest field.

The line 5789 is represented by components *d*, *e*, *f* which are spaced at about half-normal distances. "*d*" is polarized parallel, "*f*" perpendicular, and "*e*" is unpolarized. This was interpreted by Gmelin as a new type of Zeeman pattern, and it is indeed confusing without the aid of the theory. The pattern should consist of two other lines disposed symmetrically about "*d*" as "*e*" and "*f*" are, but the calculated intensities of these

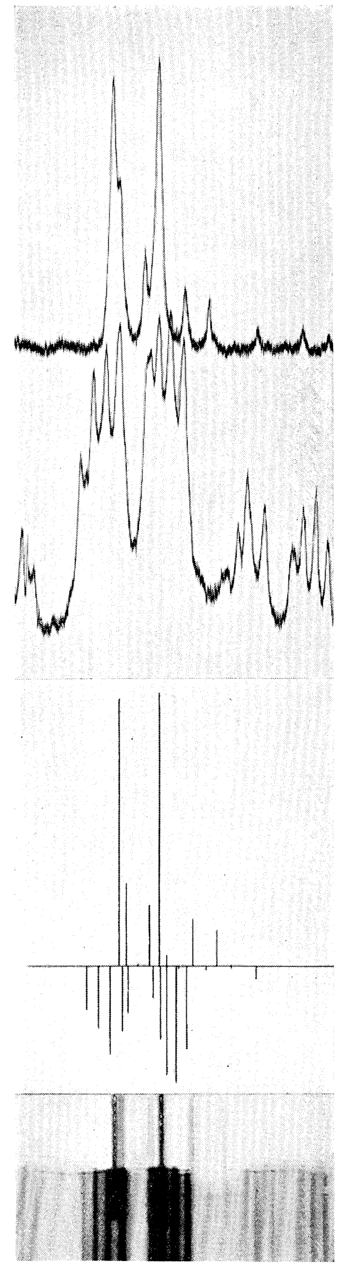

FIG. 4. λλ3662–63 at about 34,000 gauss.

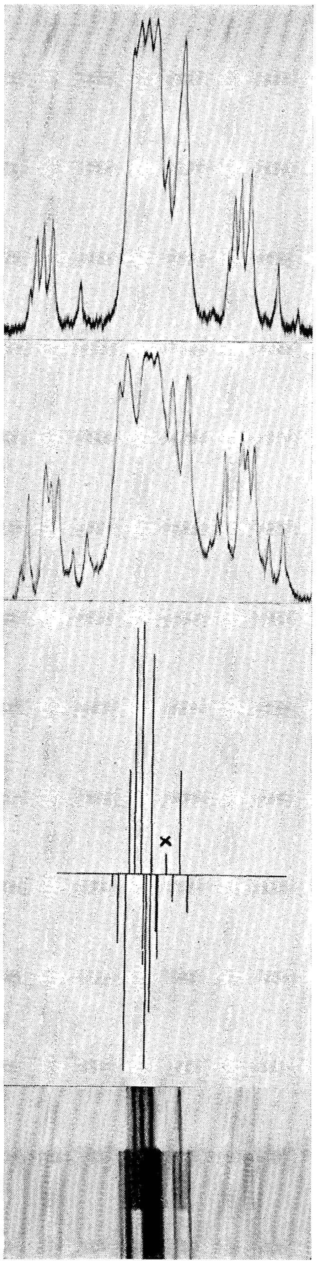

FIG. 5. λλ3131–32 at about 34,000 gauss.

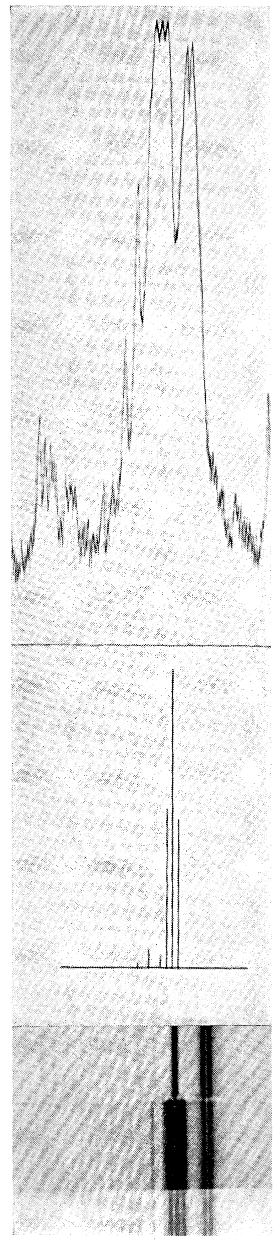

FIG. 6. λλ2967–68 at about 34,000 gauss.

lines are far below observable intensity. One of these lines is shown on the middle picture as a stub beside component "c." The agreement between theory and experiment is very satisfactory.

λλ3662–3 ($^3P_2-{}^3D_1$ and $^3P_2-{}^1D_2$)

The asymmetries introduced by the perturbations are clearly seen in Fig. 4. Here the polarizations have been separated, the parallel above and the perpendicular below, in all three pictures. The two lines are badly overlapped in the perpendicular components, only one line of λ3662 showing on the short wave side, and that is mixed in with the Rowland ghost of λ3663. Two components on the long wave side almost coincide with two components of λ3663 and show these components as doublets, visible in the photograph but not so clear in the microphotogram. Here again, the agreement is quite satisfactory.

3131–32 ($^3P_1-{}^3D_1$ and $^3P_1-{}^1D_2$)

The polarizations here have been separated as in the previous figure. Fig. 5 shows very satisfactory agreement. The component marked "x" is a usually "forbidden" component ($\Delta J=0$, $m=0\rightarrow m=0$), but it appears here with quite appreciable intensity.

2967–68 ($^3P_0-{}^3D_1$ and $^3P_0-{}^1D_2$)

Fig. 6 shows the structure of these lines. λ2968 is a transition that is usually "forbidden" ($\Delta J=2$) but is quite strong in the figure. Two different degrees of contrast are shown, together with a reversed iron line which shows the behavior of the microphotometer. The agreement is very satisfactory.

Zeeman Effects of Other Hg Lines

The Zeeman effects of several other mercury lines were also measured. The apparatus used was essentially the same as previously described[7] except that the edge of the rotating disk was kept supplied with Hg by rolling through a trough containing Hg placed on the bottom of the vacuum chamber.

The lines measured were as follows:

5770	$^1P_1-{}^3D_2$	$(\bar{0})$ (0.094) —— —— $\overline{1.213}$
5461	$^3P_2-{}^3S_1$	$(\bar{0})$ (0.504) $\overline{0.999}$ 1.508 2.010
4358	$^3P_1-{}^3S_1$	(0.518) 1.481 2.001
3650	$^3P_2-{}^3D_3$	$(\bar{0})$ (0.170) (0.345) $\overline{1.001}$ 1.177 1.346 1.507
3654	$^3P_2-{}^3D_2$	(—) $\overline{(0.771)}$ 0.718 $\overline{1.109}$ $\overline{1.494}$ 1.877
3125	$^3P_1-{}^3D_2$	$(\bar{0})$ (0.372) $\overline{0.729}$ 1.092 1.455
4916	$^1P_1-{}^1S_0$	(0) 1.013

yielding the following g-values.

						LS	Houston
$^3S_1$	2.000	2.007		Ave. = 2.003		2.000	2.000
$^1P_1$	1.025	1.013		Ave. = 1.019	Sum 2.498	1.000	1.018
$^3P_1$	1.482	1.473		Ave. = 1.479		1.500	1.482
$^3P_2$	1.512	1.495	1.503	Ave. = 1.503		1.500	1.500
$^3D_3$	1.342			Ave. = 1.342		1.333	1.333
$^3D_2$	1.109	1.119	1.101	Ave. = 1.109		1.167	1.091

If we calculate the g-values of $^1P_1$ and $^3P_1$ from Houston's formula we get $g(^1P_1)=1.018$ and $g(^3P_1)=1.482$ while the calculated g-values of $^1D_2$ and $^3D_2$ using $X=-\frac{1}{2}$ are $g(^1D_2)=1.076$ and $g(^3D_2)=1.091$.

The measuring of these lines were complicated, as mentioned, by the presence of hyperfine structure components, but in the case of lines above λ4000 these components were readily separable from the main lines, which were very much stronger. The ultraviolet lines were not so easily separated from their hyperfine structure and the results for these lines are consequently less accurate.

The measurements listed show an accuracy of 1/2 percent to 1 percent, and the authors believe, from much experience, that any attempt to list field-strength data based on Zeeman-effect measurements with a greater degree of accuracy than this is futile. Several authors have used the Zeeman effect of the mercury lines in the calculation of field strengths, especially the line λ4358, which, even well within the limits expressed above, shows a marked perturbation from the L–S pattern $\dfrac{(1)\ 3\ 4}{2}$.

[7] Green and Loring, Phys. Rev. **43**, 459 (1933).

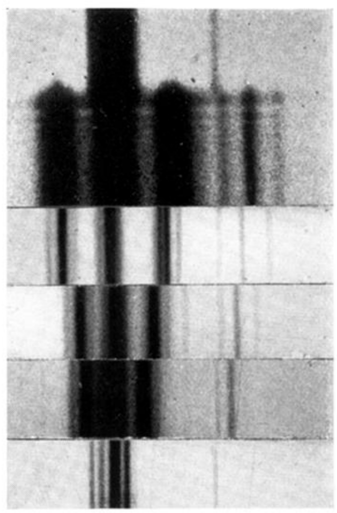

FIG. 1. λλ5789–90 at different field strengths. Hg 5789 +5790. (a) no field; (b) 34,700 gauss; (c) 29,800 gauss; (d) 21,670 gauss; (e) 16,860 gauss; (f) no field.*

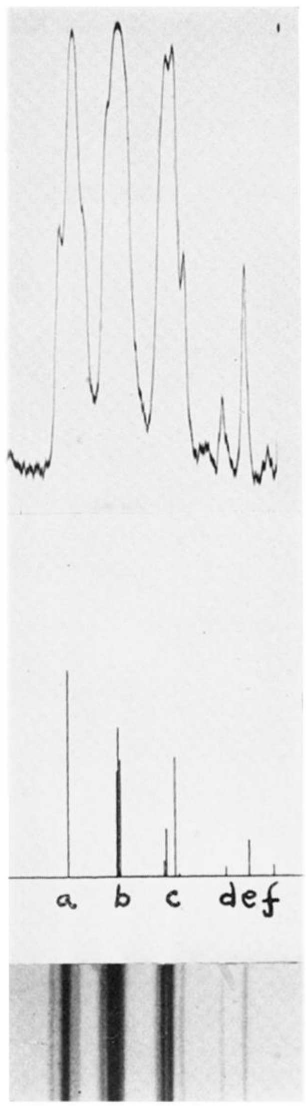

FIG. 2. $\lambda\lambda$5789–90, Field strength about 30,000 gauss.

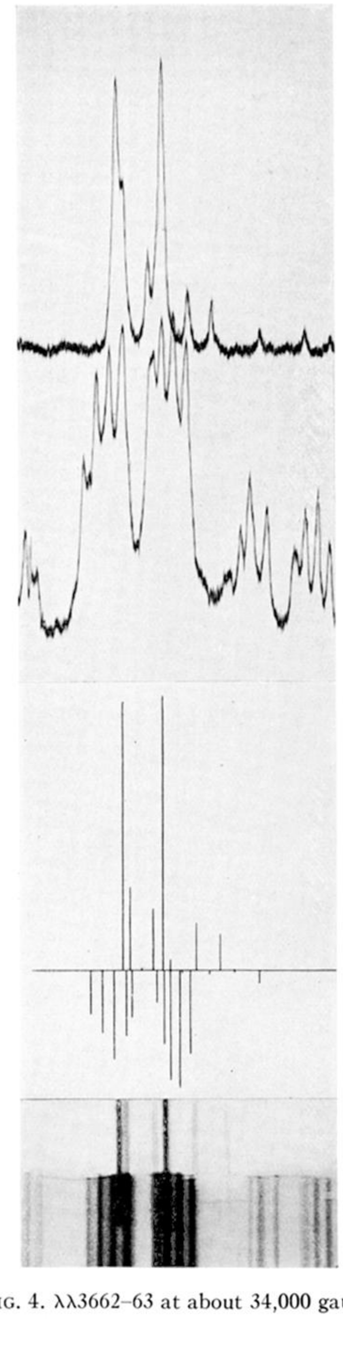

FIG. 4. λλ3662–63 at about 34,000 gauss.

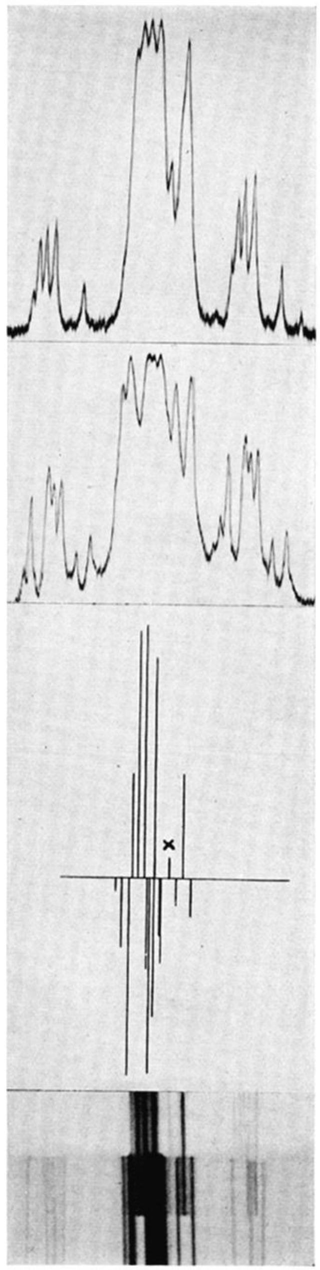

FIG. 5. $\lambda\lambda$3131–32 at about 34,000 gauss.

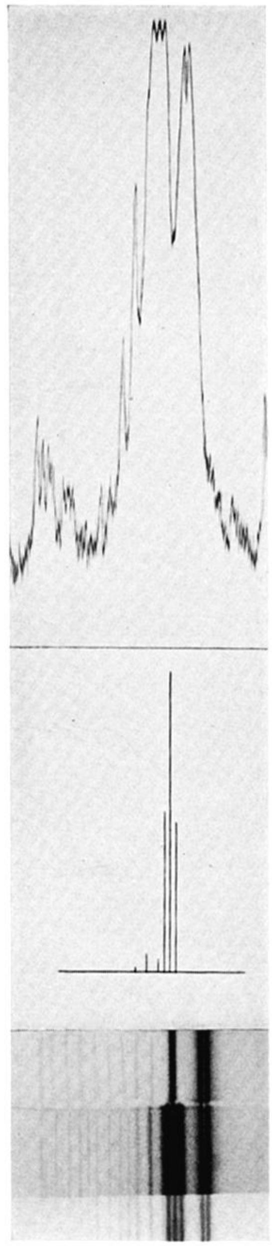

FIG. 6. $\lambda\lambda$2967–68 at about 34,000 gauss.